JOURNAL OF MATERIALS SCIENCE 15 (1980) 1709–1718

Melting behaviour and metastability of yttrium aluminium garnet (YAG) and $YAlO_3$ determined by optical differential thermal analysis

JAROSLAV L. CASLAVSKY, DENNIS J. VIECHNICKI
Army Materials and Mechanics Research Center, Watertown, Massachusetts 02172, USA

The melting point of yttrium aluminium garnet (YAG), reinvestigated by optical differential thermal analysis (ODTA), was found to be 1940 ± 7° C. Above this temperature YAG liquids are opaque, suggesting the presence of two immiscible liquids. In the composition range 10.0 to 47.5 mol % Y_2O_3, crystallization of the equilibrium phases can only occur in the presence of YAG nuclei; otherwise solidification of $YAlO_3$ and Al_2O_3 will take place. A metastable phase diagram has been defined with a metastable eutectic at 23 mol % Y_2O_3–77 mol % Al_2O_3 and 1702 ± 7° C. $YAlO_3$ (perovskite) was found to melt incongruently with a peritectic temperature of 1916 ± 7° C and a liquidus temperature of 1934 ± 7° C. $YAlO_3$ formed during metastable solidification transforms to YAG in the presence of Al_2O_3 at 1418 ± 7° C. It is suggested that the metastability arises from the difficulty of the aluminium to attain four-fold co-ordination in the YAG structure.

1. Introduction

During the course of growing large (7.5 cm diameter and 10 cm high) yttrium aluminium garnet (YAG) single crystals by vertical solidification (heat exchanger method (HEM) [1]), two crucial factors were recognized as necessary to grow single crystals free of scattering centres: (a) the starting material has to contain only the $Y_3Al_5O_{12}$ phase [2]; (b) the melting point of the garnet phase has to be known with the greatest possible accuracy in order to prevent melting of a seed crystal while simultaneously ensuring complete melting of the charge.

Published melting points of YAG are given as 1930° C [3, 4] and 1970° C [5–7]. By contrast, the temperature of thermoarrest observed during the melting of 2000 g batches of sintered YAG materials indicated that the melting point of YAG is neither 1930 nor 1970° C, but rather lies between those temperatures. In view of the conflicting information on melting points of YAG it appeared that a new determination of melting point and a study of YAG melting behaviour would be of value.

2. Measurements of the YAG melting point

At the beginning of this investigation the melting point of YAG was measured by four commonly used experimental techniques: differential thermal analysis (DTA), hot-wire microscopy, an iridium strip furnace, and direct observation of the sample melting through an optical pyrometer (DOSMTOP).

Differential thermal analysis was found unsuitable due to instability of the emf of W–3% Re versus W–25% Re thermocouple wires at temperatures over 1800° C. The melting points as determined by the hot-wire microscope, strip furnace, and DOSMTOP are listed in Table I. The average temperature 1968° C obtained by the hot-wire microscope is in good agreement with the 1970° C melting point reported by Warshaw and Roy [5], Olds and Otto [6], and Abell *et al.* [7]. On the other hand, the average melting points obtained by the other methods were too high, and a particularly large standard deviation of the DOSMTOP method measurements indicated a possible error in the concept of this method.

Despite the scatter in the YAG melting point measurements, the 2058° C melting point of

0022–2461/80/071709–10$03.00/0

TABLE I YAG melting points measurement

Sample	Hot-wire microscope (°C)	Strip furnace (°C)	DOSMTOP* method (°C)
1	1969	1987	1990
2	1969	1992	1970
3	1971	1991	1965
4	1970	1988	1974
5	1970	1975	1974
6	1971	1986	1992
7	1965	1986	1960
8	1969	1991	1962
9	1968	1990	1988
10	1968	1992	1960
11	1967	1989	1992
12	1970	1988	1996
13	1971	1990	1965
14	1968	1990	1982
15	1968	1988	1982
16	1969	1990	1988
Average	1968.94	1988.31	1978.75
Standard deviation	1.61	4.03	13.32

*Direct observation of sample melting through the optical pyrometer.

Al_2O_3 as determined by the DOSMTOP agreed well with the 2055 ± 6° C melting point reported by Jones [8] and Schneider and McDaniel [9]. Since even better agreement was found between the tabulated melting point of platinum and those measured by DOSMTOP, it was inferred that the inconsistency in the measurements of the YAG melting point was due to some intrinsic property of YAG rather than to the method itself.

Since the literature survey and results obtained show that the YAG melting point lies in the temperature range between 1930 and 1975° C, another indirect experimental method was used to better define the melting point of YAG. The method is based on Warshaw and Roy's [5] observation of the ease with which $YAlO_3$ forms from a melt of $Y_3Al_5O_{12}$ composition. The experimental arrangement was identical to that used in the DOSMTOP determination of YAG melting points with the difference that the YAG crystal was brought only to a desired temperature and cooled down. The sample was then examined by a petrographic microscope and powder X-ray diffraction analysis. Results of both examinations are presented in Table II. $YAlO_3$ was found in the sample of YAG crystal heated to 1930° C which implied that YAG started to melt at this temperature. Since the sample was held at this temperature for a short

TABLE II Microscopic and X-ray examination of YAG samples annealed at different temperatures

Blackbody enclosure temperature, (°C)	Microscopic observation	Phase present
2900	N/C*	YAG
1905	N/C	YAG
1910	N/C	YAG
1915	N/C	YAG
1920	N/C	YAG
1925	N/C	YAG
1930	N/C	YAG + trace of $YAlO_2$
1935	N/C	α-Al_2O_3 + $YAlO_3$ + traces of YAG
1940	N/C	α-Al_2O_3 + $YAlO_3$
1945	Rounding of edges	α-Al_2O_3 + $YAlO_3$
1950	Edges more rounded	α-Al_2O_3 + $YAlO_3$
1955	Sample collapsed	α-Al_2O_3 + $YAlO_3$

* No change.

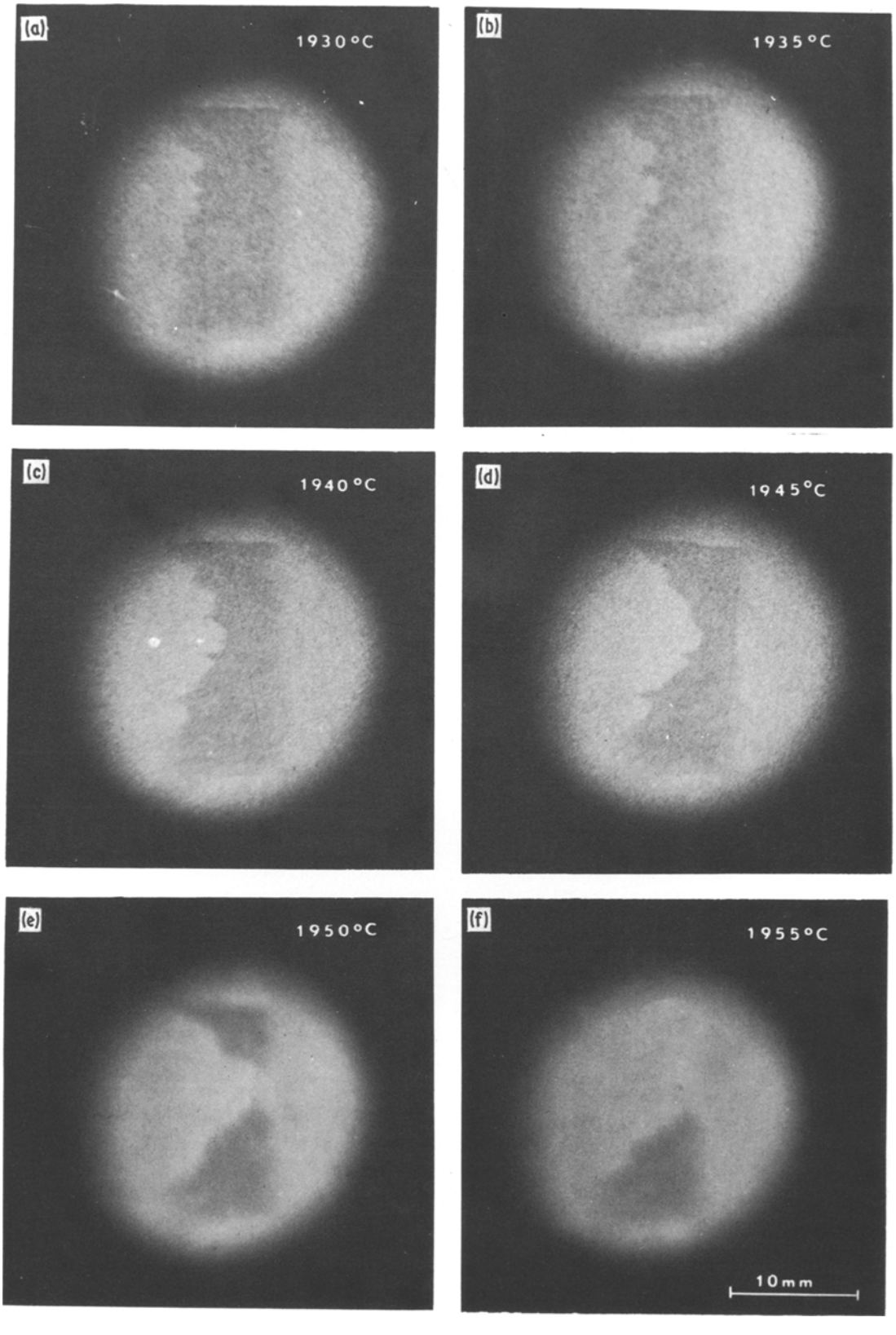

Figure 1 Photographs of the progress in melting of YAG single crystal as seen with increasing temperature.

TABLE III Measurement of brightening and darkening temperature of YAG single crystal

	Sample	Temperature (°C)	
		Brightening	Darkening
	1	1929	1934
	2	1926	2930
	3	1931	1936
	4	1927	1931
	5	1928	1934
	6	1930	1936
	7	1925	1932
	8	1927	1932
	9	1928	1936
	10	1931	1937
	11	1926	1934
	12	1929	1938
	13	1925	1937
	14	1924	1936
	15	1930	1935
Average temperature		1927.73	1934.53
Standard deviation		2.25	2.39

period of time, it was assumed that an insufficient amount of heat was supplied to the sample to achieve complete melting. To test this assumption, large samples of YAG crystals were heated as in the previous experiment except that the temperature was stabilized at a certain value measured with the optical pyrometer, which then was replaced with a camera, and the sample was photographed. This procedure was repeated for all the temperatures indicated in Fig. 1 until collapse of the sample occurred. This experiment confirmed previous findings that YAG melts or begins to melt at 1930° C and simultaneously indicated that the length of time at temperature was not the only factor determining collapse of the sample. All experiments thus far showed that the collapse of the YAG single crystal was not a sensitive indicator of the melting. Hence, a method sensitive to the change of the latent heat of melting had to be used, but for reasons previously discussed it could not employ thermocouples.

During the course of this investigation it was noticed that before the YAG crystals collapsed they first brightened and then darkened considerably. These brightening and darkening phenomena were measured and recorded in Table III for several YAG samples. The 1928° C brightening temperature was close to the 1930° C melting point of YAG reported by Toropov *et al.* [3] and Mizumo and Noguchi [4], while the 1935° C darkening temperature was near the 1937° C thermoarrest temperature observed during the melting of large boules of sintered YAG material in the crystal growth furnace; it was inferred that this optical effect was associated with the melting of YAG and also was a sensitive indicator of this melting.

3. Optical differential thermal analysis (ODTA)

Since the brightening and darkening effects of YAG are easily perceivable with the eye, it became evident that a differential curve could be registered by an optical apparatus utilizing the following radiation principles. When radiant energy strikes a material surface, part of the radiation is absorbed and part is reflected. A body which does not reflect any radiation is called a blackbody. On the other hand, at any given temperature a real object will radiate only a fraction as much energy as the blackbody and that fraction is called emissivity. Emissivity of an object varies widely with its temperature and its surface condition. In conformity with radiation principles, the optical differential curve is obtained by differentiation of current signals from two infra-red detectors. A schematic illustration is presented in Fig. 2. Detector 1 monitors the temperature of the blackbody containing the sample while the detector 2 measures the brightness temperature of the sample. The heat capacity of the blackbody enclosure 5 is considerably higher than the heat capacity of the sample 6. Accordingly, the blackbody temperature is not affected by temperature changes taking place in the sample. Therefore, the real temperature of the sample is the temperature of the blackbody enclosure. First measurements obtained by this apparatus revealed a high degree of uncertainty and indeed a real problem of how to relate maxima and minima of the ODTA curve to the temperature scale. At this point, it was realized that the infra-red detector generates a current proportional to the intensity of radiation, but that its intensity, as well as the signal current, is a highly non-linear function of the temperature. The differentiation of these mutually non-linear signals resulted in a curve with both endothermic and exothermic peaks, irregularly shaped, and often obscurred by a drift of the zero line. Linearization, 7, of the current signals with respect to the temperature prior to differentiation, 8, made the differential curve legible while simultaneously eliminating the zero drift. The ODTA record of melting an Al_2O_3 single crystal is shown in Fig. 3. Using this apparatus, melting points of 2051° C were

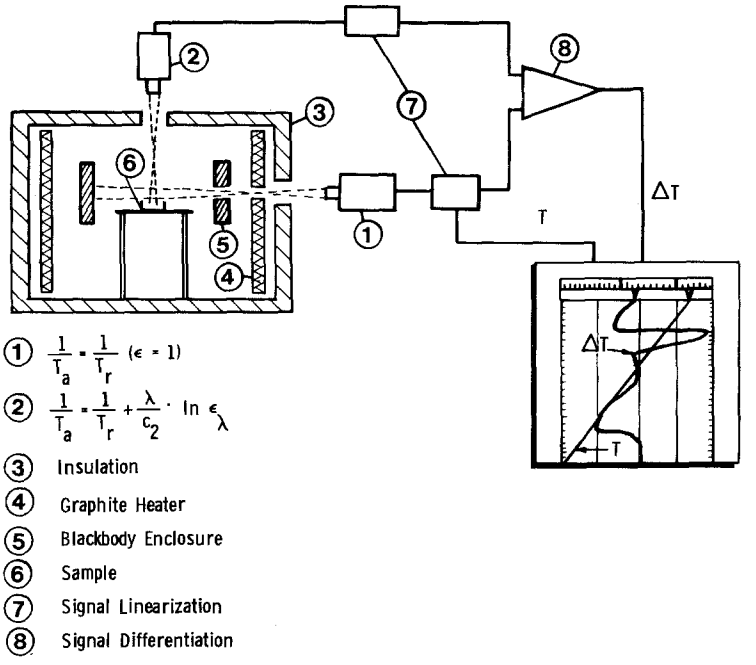

Figure 2 Schematic illustration of optical differential thermal analysis apparatus.

① $\frac{1}{T_a} = \frac{1}{T_r}$ ($\epsilon = 1$)

② $\frac{1}{T_a} = \frac{1}{T_r} + \frac{\lambda}{c_2} \cdot \ln \epsilon_\lambda$

③ Insulation

④ Graphite Heater

⑤ Blackbody Enclosure

⑥ Sample

⑦ Signal Linearization

⑧ Signal Differentiation

observed for the Verneuil-grown Al_2O_3 single crystal, 2053° C for the HEM-grown Al_2O_3 crystal, and 2056° C for the National Bureau of Standards Al_2O_3 powder. These data show good agreement with the data reported by Jones [8] and Schneider and McDaniel [9], and confirmed the suitability of the ODTA technique for determination of melting points at high temperatures.

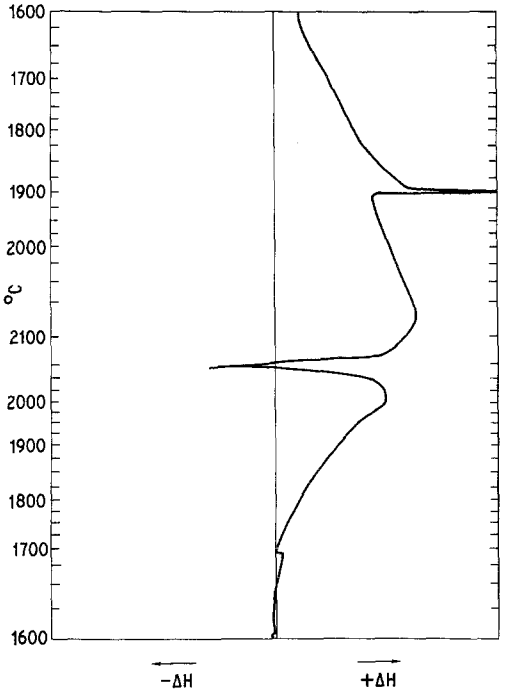

Figure 3 ODTA curve of melting and freezing of α-Al_2O_3. (NBS standard reference material no. 742.)

4. Sensitivity of the ODTA apparatus

In the final version of the ODTA apparatus, automatic optical pyrometers of the MODLINE 2000 series* are used. The current signal is linearized with respect to the temperature with a ± 10% accuracy in the range between 1200 and 2200° C. In this range the linearized output is 0 to + 100 mV d.c. The magnitude of the differential signal was evaluated experimentally from an endothermic minimum formed when a YAG crystal was heated at the rate of 7° C min^{-1}. The minimum was 32° C deep and 30° C wide. For comparison of the ODTA and DTA data, the YAG crystal was melted under the same experimental conditions, but this time a differential curve was recorded by thermocouples. The DTA endothermic minimum was only 6° C deep and 64° C wide, and indicated an approximately 30° C higher melting temperature. The better resolution of optical measurements compared to thermocouple measurements is attributed to contactless sensing of temperature, which eliminates the reaction heat loss due to the heat capacity and conductivity of thermocouples. The reproducibility of melting points as determined by the ODTA is ± 7° C in the range between 1200 and 2200° C.

*Manufactured by Ircon Inc., Skokie, Illinois, USA.

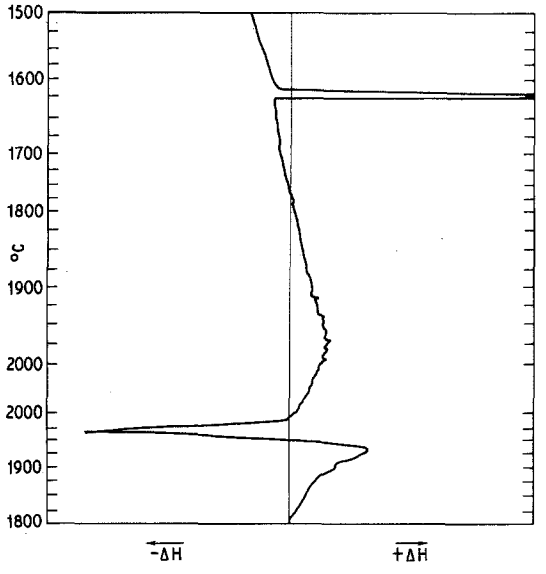

Figure 4 ODTA curve of melting and freezing of YAG single crystal.

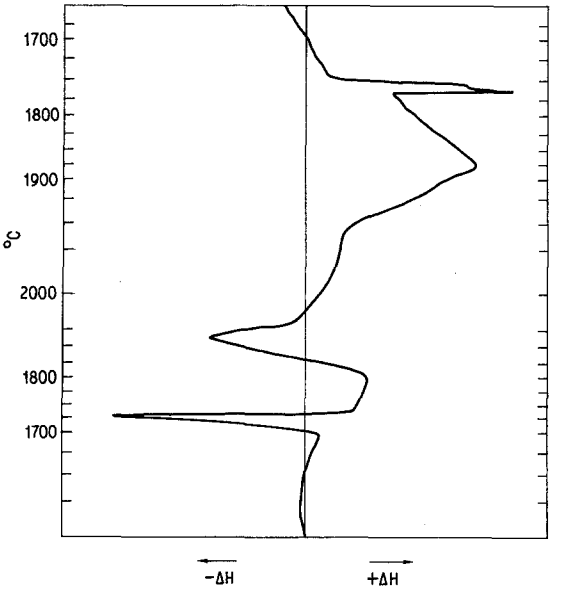

Figure 5 ODTA curve of melting and freezing of YAG; melt heated up to 2000° C and subsequently cooled to 1600° C.

5. Melting point of YAG

The ODTA curve shown in Fig. 4 depicts melting and freezing of a YAG single crystal. The first exothermic maximum at 1926° C falls in the range of the brightening of YAG which precedes its melting, as imaged by the endothermic minimum at 1939° C. With decreasing temperature, a sharp exothermic maximum at 1632° C indicates a spontaneous solidification which occurred at a high degree of supercooling. This 307° C supercooling suggests that under certain conditions the YAG melt may be able to adopt an alternative path of solidification, even though Abell *et al.* [7] considered YAG to be the only unambiguously stable phase in the Al_2O_3–Y_2O_3 system. To investigate whether the high degree of supercooling is pertinent to the YAG melt solidication or to some other phenomena, the solidified material which remained in the crucible after ODTA of YAG was subjected to a second analysis, results of which are shown in Fig. 5. Two endothermic maxima, the first at 1702° C and the second at 1855° C, substantiate the X-ray evidence which revealed that YAG, after being melted, solidifies into a mixture of Al_2O_3 and $YAlO_3$ in the absence of YAG nuclei. The minimum at 1702 ± 7° C corresponds to the temperature of the metastable eutectic formed between Al_2O_3 and $YAlO_3$, while the metastable liquidus temperature for the particular mixture is 1855° C. In an effort to define the metastable phase diagram between Al_2O_3 and $YAlO_3$, mixtures of Al_2O_3 and Y_2O_3 were reacted at 1100° C for 48 h and analysed by ODTA. The melting of samples reacted in the solid state followed the equilibrium phase diagram shown by solid lines in Fig. 6. By remelting solidified samples, the metastable diagram shown by dotted lines was defined. It should be noted that $YAlO_3$ was found to melt incongruently with a peritectic temperature at 1916 ± 7° C and a liquidus temperature at 1934 ± 7° C. Supporting data are given in Table IV.

The temperature of the metastable eutectic as determined in this work by the ODTA technique is in excellent agreement with the temperature recently published by Cockayne and Lent [10]. However, there seems to be a significant difference in the composition of the metastable eutectic. Since Cockayne and Lent [10] give no data on melting behaviour of mixtures with composition near to the composition of the metastable eutectic, it appears highly probable that they determined the composition of the metastable eutectic by the extrapolation technique. On the other hand, the composition of the metastable eutectic presented in this work was measured by the newly designed ODTA technique, sensitivity of which to small composition changes is yet to be established. Therefore, to resolve the discrepancy between Cockayne and Lent's [10] phase diagram and the one presented in Fig. 6 of this work, further

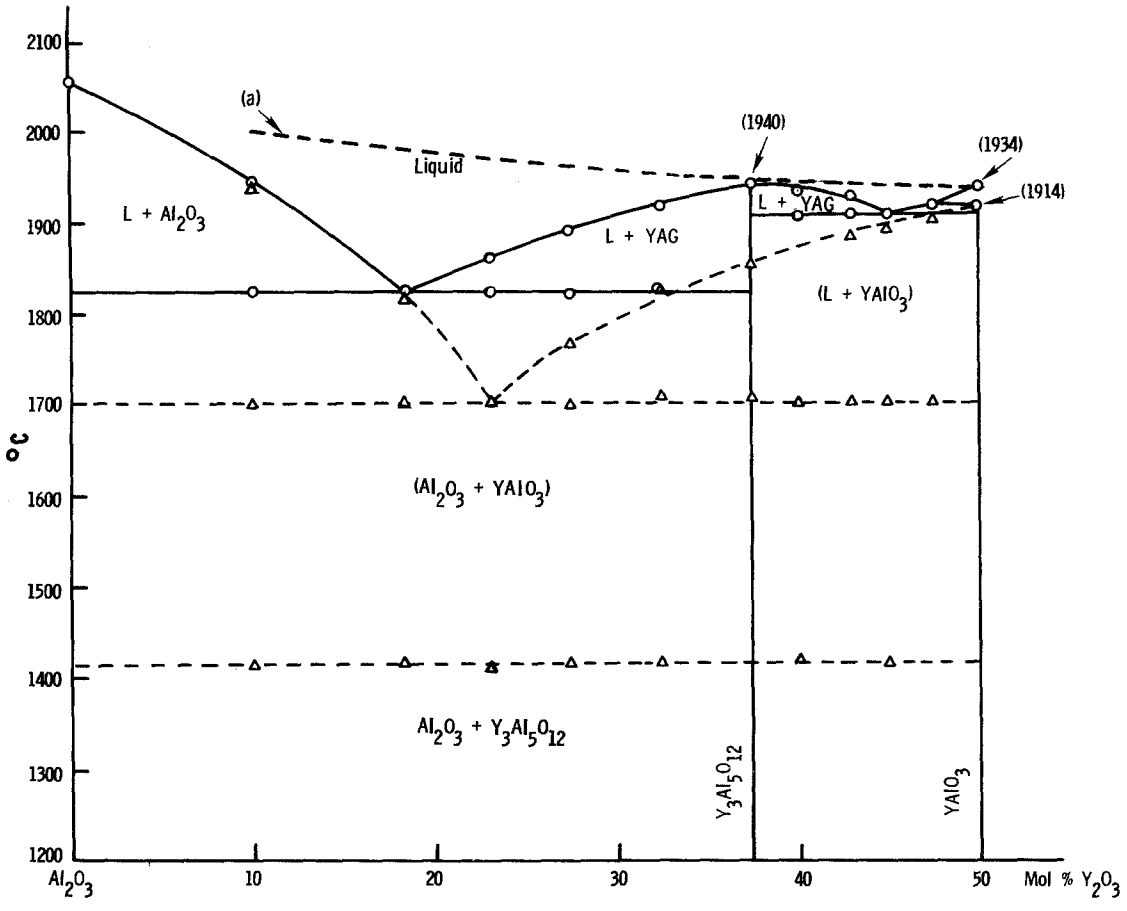

Figure 6 Phase diagram of the alumina-rich portion of the Al_2O_3–Y_2O_3 system. Equilibrium phase diagram is shown in solid lines; pertinent phase fields are labelled without parentheses. The metastable phase diagram is superimposed with dashed lines and its pertinent phase fields are labelled with parentheses. Melts heated to temperatures approximated by the dashed line (a) obey crystallization path in accordance with the equilibrium phase diagram. Melts cooled down from temperatures above the line (a) will follow metastable path of solidification.

TABLE IV Temperatures of solidus and liquidus measured by ODTA

Composition		Mixture sintered 48 h at 1100°C		Mixture melted and heated to 2000° C		Perovskite to garnet transformation (°C)
Mol% Y_2O_3	Mol% Al_2O_3	Solidus (°C)	Liquidus (°C)	Solidus (°C)	Liquidus (°C)	
10.0	90.0	1823	1942	1700	1936	1418
18.5	81.5	1826	1826	1700	1819	1419
23.0	77.0	1822	1960	1701	1701	1416
27.5	72.5	1820	1890	1698	1761	1418
32.5	67.5	1822	1914	1707	1820	1418
37.5	62.5	–	1940	1702	1855	N.M.*
40.0	60.0	1909	1933	1700	1880	1419
43.0	57.0	1909	1930	1700	1825	N.M.
45.0	55.0	1909	1909	1700	1890	1418
47.5	52.5	1909	1916	1700	1907	N.M.
50.0	50.0	1916	1934	1914	1935	–

*Not measured.

investigation of the composition of the metastable eutectic in the Al_2O_3–Y_2O_3 system is needed. Such an investigation is beyond the scope of this paper at the present time.

6. Metastability

6.1. Formation of two liquids

Observation of liquids of YAG composition during crystal growth revealed that they are always opaque, in contrast to Al_2O_3 and $YAlO_3$ melts, which are transparent. Formation of two immiscible liquids appeared to be a possible explanation of the opacity. Since the metastable eutectic has been determined between Al_2O_3 and $YAlO_3$, it was inferred that, after melting, YAG forms two immiscible liquids, Al_2O_3 and $YAlO_3$. To test this hypothesis the following experiment was conducted.

In the absence of motion, immiscible liquids with different densities will tend to stratify. In practice, however, convection currents exist which agitate the liquid. To avoid thermal agitation of the melt, the HEM technique, which minimizes convection currents because of stabilizing temperature gradients, was selected to achieve the stratification of the immiscible liquids. For this purpose, crushed YAG single crystals were melted in a cylindrical crucible in a crystal growth furnace and held for 4 h at 1990° C. After holding the melt unstirred and in thermal stable conditions for this length of time it was assumed, due to the density difference that the $YAlO_3$ melt would be situated in the lower part of the crucible where the supercooling is highest and where nucleation should occur first. To encourage localized nucleation, a heat sink of small diameter was located at the centre of the crucible bottom. After routine solidification used for growing single crystals by the HEM technique [11], the solid material was examined by X-ray Laüe method and optical microscopy. The examination revealed that the entire bottom of the crucible was covered with a single crystal of $YAlO_3$ (see Fig. 7). Since the $YAlO_3$ crystal grew from the melt of YAG composition, the constitutional supercooling instituted dendritic growth. The $YAlO_3$ dendrites shown in Fig. 8 grew in the [001] direction. The non-reacted Al_2O_3 was found as a eutectic dispersion adhering to the lower parts of the dendrites. In spite of positive results, this experiment does constitute only indirect evidence to confirm the existence of two immiscible liquids. Microscopic

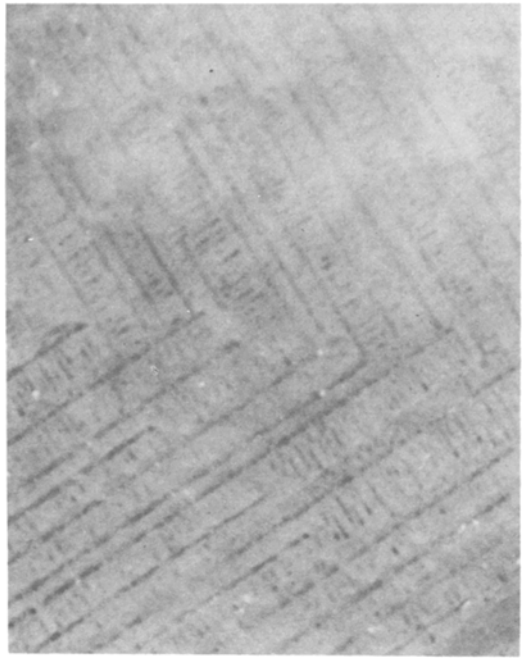

Figure 7 Perovskite twin on the bottom of $YAlO_3$ single crystal grown from the melt of $Y_3Al_5O_{12}$ composition.

examination of microstructures of metastably solidified mixtures of Al_2O_3 and Y_2O_3 ranging from 25 to 50 mol% Y_2O_3 revealed that $YAlO_3$ is always the pro-eutectic phase; hence, $YAlO_3$ will

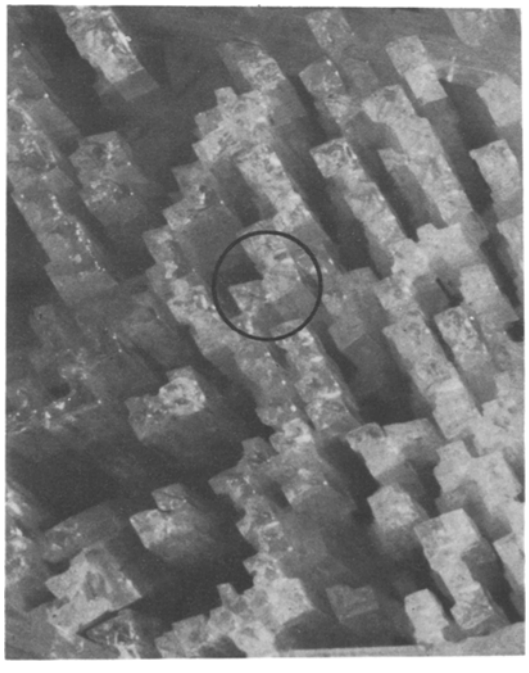

Figure 8 Dendrites finalizing the growth of the perovskite crystal shown in Fig. 7. Note the perovskite twin on tips of dendrites in circled area.

nucleate first whether the liquids are separated or not. Furthermore, study of liquids of YAG composition by ODTA up to 2050° C did not reveal any ΔH change in the melt; therefore the opacity of the YAG melt is the only evidence for existence of two immiscible liquids in the Al_2O_3–Y_2O_3 binary system.

6.2. Change of aluminium co-ordination

The fact that $YAlO_3$ melts incongruently limits its existence to temperatures below the peritectic temperature. From this point of view it is unlikely to expect the formation of two liquids, one of which has the composition of an incongruently melting compound, i.e. $YAlO_3$. Therefore, a more reasonable explanation of the preferential formation of non-equilibrium $YAlO_3$ over the YAG structure seems to lie in the fact that the aluminium has to decrease its co-ordination in order to form the garnet structure.

Aluminium–oxygen octahedra are the most important structural elements in solid and molten structures of aluminium oxide. It is not unreasonable to expect that the solid structure most similar to the short-range order of the liquid will be energetically favoured and is likely to form whether or not it is stable under the existing equilibrium conditions. As seen from Fig. 6, $YAlO_3$ (in the composition range 10.0 to 47.5 mol% Y_2O_3) transforms to YAG in solid state at 1418° C. This transformation is accompanied by the volume change evidenced by the crucible expansion (see Fig. 9), and has endothermic character which is observed by ODTA (see Fig. 10) both those effects confirm that the YAG structure has a higher energy of formation than the perovskite structure. The higher free energy of the YAG structure results from the necessity to force aluminium into a four-fold co-ordination site to form YAG.

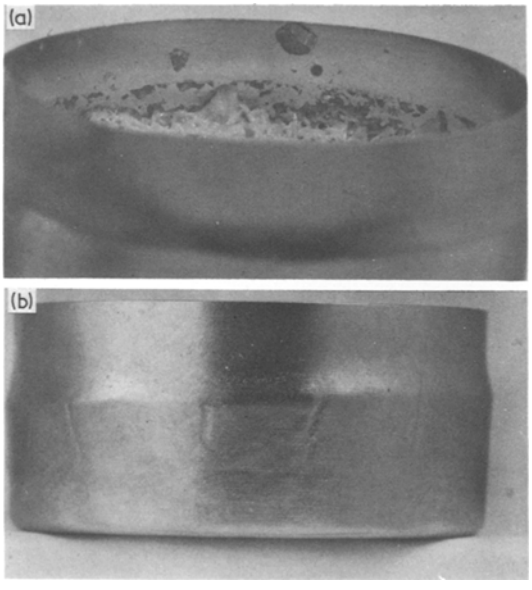

Figure 9 Photographs of the molybdenum crucible (25 mm diameter). (a) Displays relation between height of the solid with respect to deformation of crucible. (b) Wall expanded due to transformation of metastably frozen mixture of 67.5 mol% Al_2O_3 and 32.5 mol% Y_2O_3.

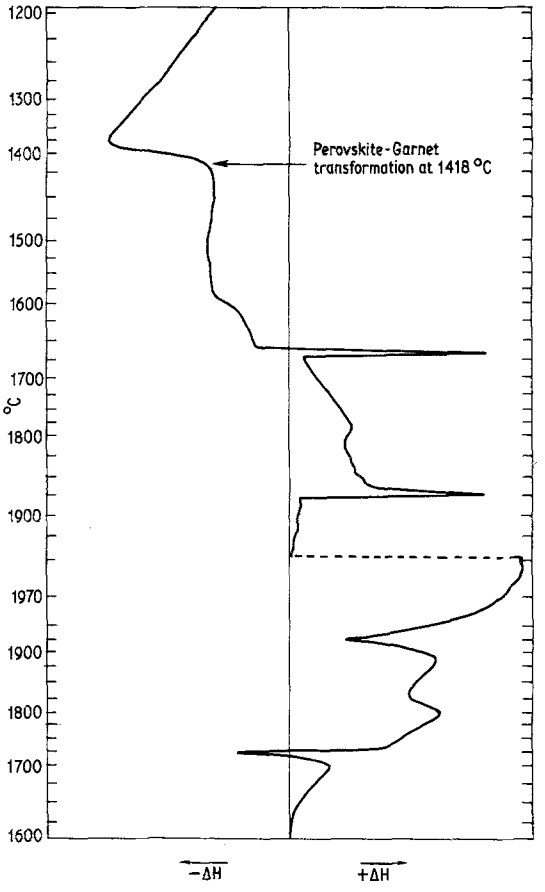

Figure 10 ODTA curve of melting and freezing of 90 mol% Al_2O_3 and 10 mol% Y_2O_3 reacted by melting.

7. Conclusions

YAG melts congruently and is stable to its melting point at 1940 ± 7° C. $YAlO_3$ (perovskite) melts incongruently with a peritectic at 1916 ± 7° C and a liquidus at 1934 ± 7° C. A metastable phase diagram was defined with a metastable eutectic at 23 mol% Y_2O_3–77 mol% Al_2O_3 and 1702 ± 7° C. $YAlO_3$ formed during metastable solidification transforms to YAG in the presence of Al_2O_3 at 1418 ± 7° C.

When melt temperatures do not exceed 1940° C, the melts of Y_2O_3 and Al_2O_3, ranging in composition from 10 to 45 mol% of Y_2O_3, retain aluminium in four-fold co-ordination; therefore, they obey the crystallization path of the equilibrium phase diagram. However, at approximately 2000° C a structural change takes place in the liquid; consequently the melts, cooled down from temperatures above 2000° C, follow the crystallization path of the metastable phase diagram. The metastability is due to the fact that aluminium prefers the six-co-ordination in the melt, which also explains the difficulty of growing YAG single crystals from melt, since the growth rate is predominantly controlled by the rate of a decrease in the aluminium co-ordination.

Furthermore, recent studies of Al_2O_3–Nd_2O_3–Y_2O_3 ternary phase relations by ODTA indicate that neodymia destabilizes the four-fold co-ordination of aluminium, which increases the difficulty in growing Nd:YAG single crystals of laser quality.

Acknowledgements

The authors are indebted to Dr R. Roy and Dr W. B. White for their critical reading of the manuscript and constructive suggestions, and to W. Earle for his valuable assistance with the experimental aspects of this work.

References

1. D. J. VIECHNICKI and F. SCHMID, *J. Crystal Growth* **26** (1974) 162.
2. D. J. VIECHNICKI and J. L. CASLAVSKY, Army Materials and Mechanics Research Center, AMMRC TR 78-7, February 1978. *Amer. Ceram. Soc. Bull.* (1979).
3. N. A. TOROPOV, I. A. BONDAR, F. Ya. GALADHOV, Kh. S. NIKOGOSYAN, and N. V. VINOGRADOVA, *Izv. Akad. Nauk. SSSR Ser. Khim.*, 7 (1969) 1158.
4. M. MIZUMO and T. NOGUCHI, *Rep. Gov. Ind. Res. Inst. Nagoya* **16** (1967) 171.
5. I. WARSHAW and R. ROY, *J. Amer. Ceram. Soc.* **42** (1959) 434.
6. L. E. OLDS and H. E. OTTO, "Phase Diagrams of Ceramists", edited by E. M. Levin, *et al.* (J. Amer. Cer. Soc., 1969) Fig. 311.
7. J. S. ABELL, J. R. HARRIS, B. COCKAYNE, and B. LENT, *J. Mater. Sci.* **9** (1974) 527.
8. T. P. JONES, *J. Aust. Ceram. Soc.* **5** (1969) 41.
9. S. J. SCHNEIDER and C. L. McDANIEL, *J. Res. Nat. Bur. Stand.* **71A** (1967) 317.
10. B. COCKAYNE and B. LENT, *J. Crystal Growth*, **46** (1979) 371.
11. J. L. CASLAVSKY and D. J. VIECHNICKI, *ibid* **46** (1979) 601.

Received 28 September and accepted 20 November 1979.